

Plane wave excitation by taper array for optical leaky waveguide antenna

Hiroshi Hashiguchi^{a)}, Toshihiko Baba, and Hiroyuki Arai

Graduate School of Engineering, Yokohama National University,

79–5, Tokiwadai, Hodogayaku, Yokohama-city, Kanagawa 240–8501, Japan

a) hashiguchi-hiroshi-cn@ynu.jp

Abstract: This paper proposes and demonstrates a plane-wave generator which consists of a compact taper array and expands the aperture of the grating waveguide (GWG) of optical leaky wave antenna, resulting in a high antenna gain. The device size is reduced to half of a conventional slow taper without degrading the aperture efficiency. We confirm the well correspondence of the antenna gain between the full numerical simulation and the estimation using measured parameters for the device fabricated by silicon photonics.

Keywords: optical antenna, leaky wave, silicon photonics, beam scanning, optical mobile communication, grating waveguide

Classification: Integrated optoelectronics

References

- [1] J. Sun, *et al.*: “Two-dimensional apodized silicon photonic phased arrays,” *Opt. Lett.* **39** (2014) 367 (DOI: [10.1364/OL.39.000367](https://doi.org/10.1364/OL.39.000367)).
- [2] D. Kwong, *et al.*: “On-chip silicon optical phased array for two-dimensional beam steering,” *Opt. Lett.* **39** (2014) 941 (DOI: [10.1364/OL.39.000941](https://doi.org/10.1364/OL.39.000941)).
- [3] D. N. Hutchison, *et al.*: “High-resolution aliasing-free optical beam steering,” *Optica* **3** (2016) 887 (DOI: [10.1364/OPTICA.3.000887](https://doi.org/10.1364/OPTICA.3.000887)).
- [4] K. Van Acoleyen, *et al.*: “One-dimensional off-chip beam steering and shaping using optical phased arrays on silicon-on-insulator,” *J. Lightwave Technol.* **29** (2011) 3500 (DOI: [10.1109/JLT.2011.2171477](https://doi.org/10.1109/JLT.2011.2171477)).
- [5] A. Yaacobi, *et al.*: “Integrated phased array for wide-angle beam steering,” *Opt. Lett.* **39** (2014) 4575 (DOI: [10.1364/OL.39.004575](https://doi.org/10.1364/OL.39.004575)).
- [6] H. Hashiguchi, *et al.*: “An optical leaky wave antenna by a waffled structure,” *J. Lightwave Technol.* **35** (2017) 2273 (DOI: [10.1109/JLT.2017.2660520](https://doi.org/10.1109/JLT.2017.2660520)).
- [7] K. Van Acoleyen, *et al.*: “Two-dimensional dispersive off-chip beam scanner fabricated on silicon-on-insulator,” *IEEE Photonics Technol. Lett.* **23** (2011) 1270 (DOI: [10.1109/LPT.2011.2159785](https://doi.org/10.1109/LPT.2011.2159785)).
- [8] G. Roelkens, *et al.*: “Grating-based optical fiber interfaces for silicon-on-insulator photonic integrated circuits,” *IEEE J. Sel. Top. Quantum Electron.* **17** (2011) 571 (DOI: [10.1109/JSTQE.2010.2069087](https://doi.org/10.1109/JSTQE.2010.2069087)).
- [9] X. Chen and H. K. Tsang: “Polarization-independent grating couplers for silicon-on-insulator nanophotonic waveguides,” *Opt. Lett.* **36** (2011) 796 (DOI: [10.1364/OL.36.000796](https://doi.org/10.1364/OL.36.000796)).
- [10] S. Kinugasa, *et al.*: “One-chip integration of optical correlator based on slow-

light devices,” Opt. Express **23** (2015) 20767 (DOI: 10.1364/OE.23.020767).
[11] [Online]. Available: www.cst.com CST Microwave Studio.

1 Introduction

Grating waveguides (GWGs) and optical phased arrays have attracted attention as optical antennas toward next era high-speed optical wireless communication and other advanced applications such as light detection and ranging [1, 2, 3, 4, 5]. The GWGs are a type of optical leaky waveguide antennas (OLWAs), which gradually radiate a guided mode to free space by the refractive index perturbation of the periodic linear grating. In general, for any antennas, a high antenna gain is crucial for sharp beam forming, while it requires a large antenna size. For GWGs, the effective aperture size is evaluated not by the physical size but by the radiation aperture. In the longitudinal direction along the waveguide, the effective aperture is inversely proportional to the magnitude of the index perturbation; it is extended by employing a shallow grating and/or a waffle structure [6, 7]. In the lateral direction across the waveguide, the core of the GWG is widened to enhance the antenna gain. In this case, a problem is how to excite a plane wave (precisely speaking, a plane-wave-like single peak wave) in the widened core of the GWG to maintain a high aperture efficiency and achieve a high antenna gain. Usually, a tapered waveguide is put in front of the such a GWG to excite the plane wave. However, when the GWG is much wider than input waveguide and wavelength of the light, the taper must be sufficiently slow and adiabatic, which makes the taper very long. For example, in the experiment shown later, the initial waveguide width is $0.4\ \mu\text{m}$ and final width is $20\ \mu\text{m}$, meaning an expansion ratio of 50. To maintain the adiabatic transition, the taper length becomes $200\ \mu\text{m}$ in the case of simple taper, meaning a taper length to final width ratio of 10. If the final width is enhanced further to, e.g., $100\ \mu\text{m}$, the taper length will be 1 mm, which too long as just a mode converter in dense photonic circuits. Moreover, the excitation of the ideal plane wave is not so robust when the taper becomes too long, because slight structural disordering in the fabricated device easily excites unwanted profiles.

In this paper, we propose to use a compact taper array with a power divider instead of a single long slow taper for producing the plane wave. We succeed in demonstrating a high antenna gain without disordering the plane wave excitation and degrading the aperture efficiency in both simulation and measurement. The detail of the proposed device structure and its theoretical characteristics are shown in Section 2. The comparison between the estimation using measured parameters for fabricated device and full numerical simulation are shown in Section 3. Section 4 gives the conclusion.

2 Fabricated condition and geometry

Fig. 1 shows design parameters of the GWG with the taper array that we propose and actually fabricated using silicon photonics technology. The wavelength band targeted is $\lambda = 1.50\text{--}1.60\ \mu\text{m}$. The GWG, taper and dividers are all formed in a

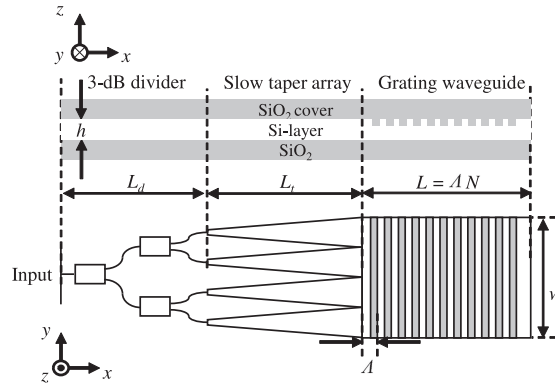


Fig. 1. Schematic and design parameters of GWG with taper array. We set $h = 0.21 \mu\text{m}$, $L_d = 42 \mu\text{m}$, $L_t = 50 \mu\text{m}$, $w = 20 \mu\text{m}$, $\Lambda = 0.54 \mu\text{m}$ and $N = 100$.

Si-layer (thickness $h = 0.21 \mu\text{m}$) buried by silica (SiO_2) claddings. The refractive index of Si and SiO_2 are 3.45 and 1.45, respectively. The depth of the grating also formed on top of the Si-layer is suppressed to 10 nm to moderate the index perturbation. The GWG radiates upward and downward beams. It would be possible to suppress the downward radiation by introducing a bottom reflector [8]. However, we neglected it in this study due to the constraints in our fabrication process and measurement setup. The GWG radiates a light beam to the direction θ , satisfying the phase matching condition between the free space and the propagation constant of the guided mode, which is determined by the etching depth d , waveguide width w , and pitch Λ . We set Λ at $0.54 \mu\text{m}$ to obtain θ from 0 to -10° within the target wavelength band. Here, the radiation $\theta = 0^\circ$ along the z -axis becomes weak due to the Bragg condition [9]. In general, the antenna gain G in the units of dBi is proportional to the aperture size $A = wL$, and the relation between them is expressed as follows:

$$G = \frac{4\pi A}{\lambda^2} \eta \quad (1)$$

where η is the aperture efficiency, which does not exceed 50% due to the existence of the downward radiation. To simulate a high antenna gain, we have to make the size of the GWG as long and wide as possible, but it is very time consuming. For a moderate simulation time, we set the length $L = 54 \mu\text{m}$ (the number of the grating lines $N = 100$) and the width $w = 20 \mu\text{m}$ for the grating, and also set the taper length at $200 \mu\text{m}$ in the case of the conventional single taper. For the purpose of exciting a plane wave in a wide GWG by a short taper structure without degrading the aperture efficiency, we divide the original single taper into, e.g., four smaller tapers, keeping the length to width ratio. The final width of the divided slow tapers is $5 \mu\text{m}$. Then the size of the taper array becomes $50 \times 20 \mu\text{m}^2$. We add a 1×4 power divider consisting of three 1×2 multi-mode interference dividers [10] each connected by Si wire waveguides of $0.4 \mu\text{m}$ width. The total device size is $92 \times 20 \mu\text{m}^2$ which is a half size of conventional single taper, even including the dividers. Fig. 2 shows the normalized electrical field distribution at the input edge of the GWG and the comparison of the radiation pattern inside the zx -plane, which are calculated by using three-dimensional (3D) full-wave commercial simulator

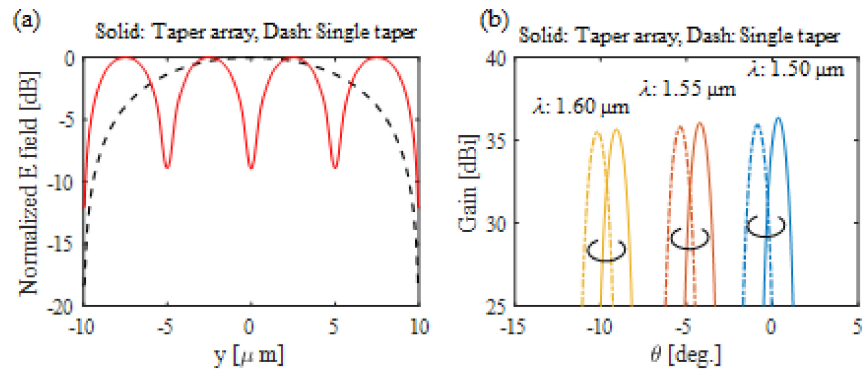


Fig. 2. (a) Electrical field distribution at the input edge of the GWG with $\lambda = 1.55 \mu\text{m}$, (b) Radiation patterns simulated for proposed four-taper array and conventional slow taper in the zx -plane.

CST MW Studio [11]. The normalized electrical field distribution of the proposed structure exhibits multi peak profile, which correspond to the number of small tapers as shown in Fig. 2(a). The taper array exhibits an antenna gain value which is almost comparable to that of a single slow taper in the entire wavelength range of this simulation as shown in Fig. 2(b). The slight difference of the radiation angle between them might be caused by the finite mesh size, which barely deforms the model. Our simulation software automatically decides the mesh size, which is slightly changed by the entire size of modeling, even though we employ the same settings. We are not able to find the optimal setting because how to create the mesh is not disclosed. In addition, the fabrication error and measurement error, which slightly change the beam direction, might occur. Anyway, this difference is not serious in discussing the antenna gain of these devices.

3 Experimental results and comparison

Fig. 3 shows the blueprint and top view of fabricated devices including the proposed taper array waveguide and the GWG. The fabricated devices had the GWG with slightly different parameters to compensate the fabrication errors, as

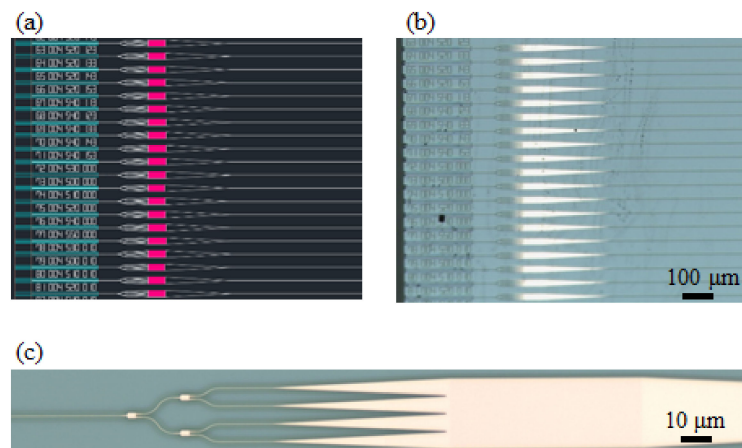


Fig. 3. Fabricated devices. (a) CAD blueprint for fabricated chip (b) Magnified top view of fabricated (c) Magnified GWG that we can confirm the periodic linear grating.

shown in Fig. 3(a) and (b). These devices were fabricated by using 200 mm-diameter silicon-on-insulator and complementary metal oxide semiconductor process with KrF excimer exposure. The detailed structural parameters of the GWG were the same as those shown in Section 2. The size of the taper array including the 1×4 divider was $92 \times 20 \mu\text{m}^2$. We can see that it is half of the conventional single slow taper ($200 \times 20 \mu\text{m}^2$) connected to the GWG on the right side. The radiation pattern was observed by using a microscope equipped with infrared InGaAs camera and optical power meter. The beam orientation was changed by sweeping incident wavelength, and its angle θ was measured by defocusing the near field pattern, as shown in Fig. 4(b). We only show the near field pattern at $\lambda = 1.55 \mu\text{m}$ because the wavelength dependence of near field pattern was small.

The far field patterns observed from the near field on the defocused plane are shown in Fig. 4(d). The GWG radiated a beam in the range from $\theta = 0^\circ$ to -10° for $\lambda = 1.5$ to $1.6 \mu\text{m}$, which agrees well with the simulation. Since there are no standard antennas in optical antenna measurements, such as dipole antennas in RF measurements, we estimated the antenna gain of the GWG by using the surface aperture distributions method (ADM) [6], which approximates the aperture distribution via the following equations,

$$E(x, y) = E_0 |\sin(4\pi(y/w))| \exp(-\alpha + j\beta)x \quad (2)$$

$$\beta = k_0 \sin \theta \quad (3)$$

$$D(\theta, \phi) = \int_0^w \int_0^L E(x, y) \exp jk_0(x \sin \theta \cos \phi + y \sin \theta \sin \phi) dx dy \quad (4)$$

where α is the radiation decay factor and β is the wave number. The radiation decay factor is estimated by measuring the surface power distribution, as shown in Fig. 4(d). The slope evaluated by the least mean square method gives $\alpha = 0.17 \text{ dB}/\mu\text{m}$. The wave number is approximated from the measured θ and Eq. (3). We substituted these parameters into Eqs. (2) and (4) to calculate the aperture distribution and radiation pattern. Such estimation results are compared with that obtained by the CST simulation in Fig. 5. The reduction in the measured gain at $\lambda = 1.5 \mu\text{m}$ might be caused by the influence of the Bragg condition mentioned in Section 2. The gain values of other wavelengths show good agreement within a $\pm 0.5 \text{ dB}$ error. The difference of the radiation angle might be caused by a measurement error. Anyway, we confirmed from this result that the taper array is effective as a compact plane-wave generator, which maintains the aperture efficiency comparable to that in the conventional single slow taper.

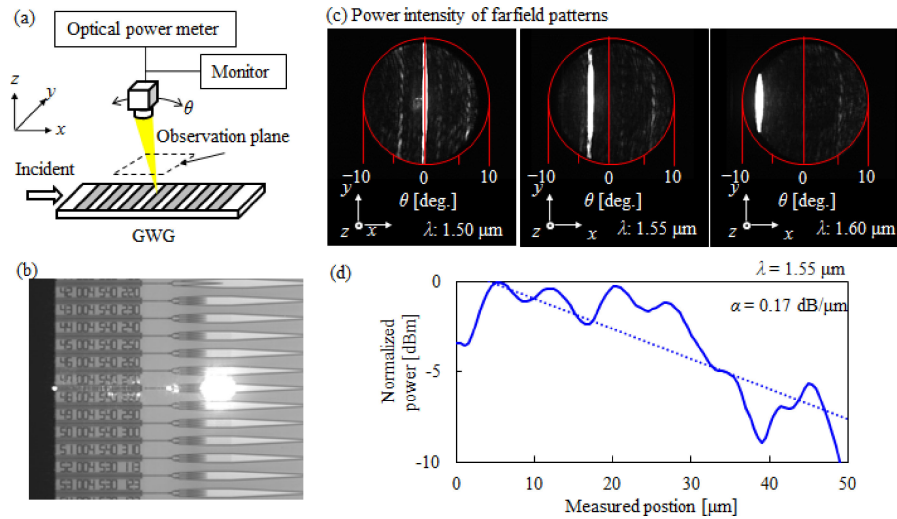


Fig. 4. Measurement results of far-field pattern of radiated optical beam from GWG with four-taper array. (a) Measurement setup. (b) Near field pattern. (c) Far field patterns (d) Measured power distributions along the GWG at near field, which gives the radiation decay factor.

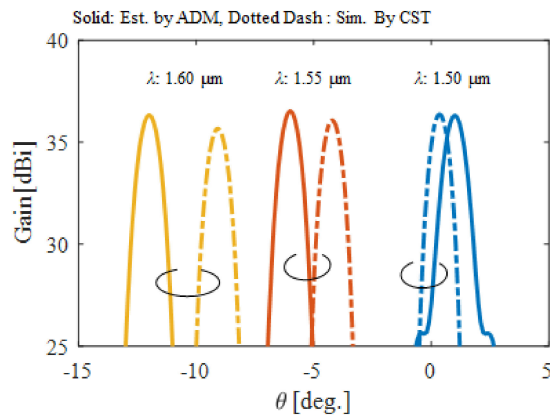


Fig. 5. Comparison of directivity between the estimation by ADM and simulation by CST MW Studio.

4 Conclusion

We proposed the taper array plane-wave generator in front of the widened GWG, which consists of compact divided tapers. Its size was half of the conventional single slow taper even including additional optical power divider. We compared the antenna gain between the simulation and measurement, and confirmed a good agreement. This structure will help the excitation of much wider plane-wave in optical antennas to further enhance the antenna gain.